A Multi-scaled Analysis of Forest Structure using Individual-Based Modeling in a Costa Rican Rainforest

A. H. Armstrong[1,2], A. Huth[3, 6], B. Osmanoglu[4], G. Sun[4, 5], K. J. Ranson[4], R. Fischer[3,7]

1 Universities Space Research Association, Columbia, Maryland, USA
2 University of Virginia, Dept. of Environmental Sciences 290 McCormick Road Charlottesville, VA 22903, USA
3 Department of Ecological Modelling, Helmholtz Centre for Environmental Research–UFZ, Permoserstr. 15, 04318, Leipzig, Germany
4 NASA/Goddard Space Flight Center, Biospheric Sciences Laboratory, Greenbelt, MD, USA
5 Department of Geographical Sciences, University of Maryland, College Park, MD, USA
6 University of Osnabrück, Institute of Environmental Systems Research, Barbarastr. 12, 49076 Osnabrück, Germany
7 German Centre for Integrative Biodiversity Research (iDiv) Halle-Jena-Leipzig, Deutscher Platz 5e, 04103 Leipzig, Germany

Abstract:

Consideration of scale is essential when examining structural relationships in forests. In this study, we present a parameterization of the FORMIND individual-based forest model for old growth Atlantic lowland rainforest in La Selva, Costa Rica. Results show that the simulated forest reproduces the structural complexity of Costa Rican rainforest within 2.3% of aboveground biomass values, based on comparisons with CARBONO inventory plot data. The Costa Rica FORMIND simulation was then used to investigate the relationship between canopy height and aboveground biomass (AGB), leaf area index (LAI) and gross primary productivity (GPP) at different spatial scales (20x20m, 60x60m, 100mx100m). The relationship between aboveground biomass and height is of particular importance toward the calibration of various remote sensing products including lidar and radar, whereas the LAI and GPP relationships are understudied in this context. We found that the relationship between all three variables and height varies considerably: the relationship is stronger at finer scales and weaker at coarser resolution. However, in all three comparisons, RMSE also decreased as scales coarsened, with the largest difference shown between 100m and 10m resolutions in relating AGB to Lorey's height (R^2 decreased by 0.3; RMSE decreased by 114.5 Mg/ha). This suggests that a trade-off between accuracy and precision exists, and further highlights the importance of spatial scale in determining the relatability of forest structure variables.

Introduction

The accurate measurement of forest structure variables is essential in understanding forest function at multiple spatial scales. Forest attributes like aboveground biomass (AGB) are crucial components of studies in global change and carbon cycling (Chave et al. 2003; Dixon et al. 1994; Drake et al. 2002; Lefsky et al. 2002; Perry 1994; Saatchi et al. 2011a). Directly measured variables (e.g. diameter at breast height (DBH), tree height, basal area, leaf area index and stem counts) are achieved at either the individual tree or the plot level, whereas forest attribute variables (e.g. aboveground biomass, net primary productivity, etc.) can only be estimated from these direct measurements by applying equations and in some cases through time to calculate rates. Forest models aid in understanding these relationships between forest structure and other forest variables. Since the 1970s, individual-based gap models (IBGM) have successfully elevated our knowledge of forest dynamics, especially across temperate and boreal forested landscapes (Botkin et al. 1972; Bugmann 2001; Kohler and Huth 1998; Shugart 1984, 1998, 2003, 2018). The versatility of IBGMs allows for high precision scaling of the amalgamation of direct-measurement plot data to landscape level calculations of changes in indirect measures, such as forest productivity and carbon flux.

Particularly in the tropics, where ecosystem complexity is high and the forests themselves are often hard to reach, there is a general lack of long-term repeated forest inventory datasets. This has hindered the advancement in the understanding of the dynamic floral and structural complexities found in these ecosystems. Over recent decades, IBGMs have been used to fill this knowledge gap in understanding the mechanisms that underlie growth, mortality and recruitment within tropical forest ecosystems (Fischer et al. 2016; Fischer et al. 2014; Hurtt et al. 2010; Huth et al. 2005; Kohler and Huth 2007; Kohler et al. 2003). IBGMs have already been used to understand different aspects of tropical forests in a changing world, including: succession, structural dynamics, species competition and many other mechanisms that underlie long-term dynamics (Botkin et al. 1972; Bugmann 2001; Fischer et al. 2016; Pretzsch 2009; Shugart 1998, 2003, Armstrong et al 2018).

The well-documented rainforest of La Selva, Costa Rica provides a unique opportunity to examine how productivity, aboveground biomass and carbon flux varies through time and space. Costa Rican rainforests are among 25 global biodiversity hotspots that comprise 44% of the world's plant species within 1.4% of the land area (Myers et al. 2000). La Selva is a notable exception to the lack of long-term datasets that have hampered research efforts elsewhere. The core of the research station property was purchased by the Organization for Tropical Studies (OTS) in 1968 and surrounding parcels were purchased into the early 1990s to form the current 1,536ha protected area. There exist much knowledge about the history of human intervention and inhabitance for this region up to 3000 Y.B.P., as confirmed by carbon dating buried charcoal (McDade et al., 1994). The successional state of the forests within the research area is therefore relatively well-known.

Launched in 1996 by D.A. Clark, D.B. Clark and S.F. Oberbauer, the CARBONO Project has carried out annual forest measurements in 18 x 0.5ha plots located across the biological station, including relatively fertile flat sites on old alluvial soils, infertile flat sites on ridge tops, and infertile steep slopes (Clark and Clark 2000). Additionally, studies scaling structural dynamics and productivity to the landscape level, utilizing techniques combining long term plot data, remote sensing and forest modeling have contributed to an in-depth knowledge of La Selva's rainforest (Drake et al. 2002, Dubayah 2010; Hurtt 2004; Tang 2012). Drake et al. (2002) validated the use of a large-scale footprint lidar (LVIS) to capture forest structure variables across multiple landcover types, including pasture, secondary and primary tropical forests. LVIS metrics were able to predict field derived quadratic mean stem diameter, basal area and AGB. Similarly, Dubayah et al. (2010) and Tang et al. (2012) used LVIS to detect changes in canopy structure over La Selva between 1998 and 2005 by relating observed

changes in canopy height, other height metrics and biomass to field derived changes (Dubayah), and vertical transects of leaf area index (Tang). Hurtt et al. (2004) used airborne lidar observations to initialize the Ecosystem Demography Model. Their results produced 1ha-resolution biomass maps that showed increased model prediction accuracy when initialized with LVIS, and compared findings to known forest types within La Selva.

Utilizing a higher resolution modeling framework (e.g. IBGMs) provides the potential for directly connecting with high resolution remotely sensed datasets at a user-defined scale. With the advances of supercomputer capabilities during the last decade, IGBMs are poised to not only be initialized with high resolution remote sensing datasets as with Hurtt et al.'s study, but to produce maps that broaden the spatial and temporal scale from existing satellite imagery, with unprecedented accuracy. However, when using satellite imagery, field-based studies and IGBMs to answer scientific questions, it is important to consider the spatial scale at which each operates, as well as how each measures structure variables. It is not yet fully understood how strongly forest structure correlates with other desired forest variables (e.g., AGB) and how strong the influence of the spatial scale is on this relationship. On a finer scale (e.g. 20m) the forest structure can be better described, but the estimation of forest variables like aboveground biomass becomes very uncertain (e.g., due to edge effects and uncertainties in allometries). On coarser scales (e.g. 100m) these estimate become more reliable, but the fine-scale details of forest structure cannot taken into account. The choice of a suitable spatial scale is an important question, especially in remote sensing. Therefore, our study addressed the following research question:

How does the crucial relationship between canopy height metrics and forest stand biomass (AGB), leaf area index (LAI) and gross primary productivity (GPP) change at different spatial resolutions?

This question should be answered by linking extensive field data with a forest model. Given the substantial knowledge base, La Selva's rainforest is ideal for examining the use of individual-based gap models and the veracity of remote sensing derived structure variables. The model FORMIND was applied in the study to reproduce the patterns found in old growth tropical forest at La Selva Biological Station. Specifically, we compared distributions in the number of trees, basal area, aboveground biomass and the stem size distribution of the modeled forest to that of the La Selva forest inventory dataset. To ensure that our analysis was not biased by how we defined canopy height, we made comparisons based on four standard height definitions, including: the mean tree height (Mean), lidar derived maximum height (RH100), canopy height (Canopy) as defined by Kohler and Huth (2010) and mean height weighted by basal area (Lorey's Height). In this manuscript, we present our three forest variables (AGB, LAI and GPP) compared to Lorey's Height. The same comparisons to RH100, Canopy height and Mean tree height can be found in the supplementary Appendices.

Methods

Field site Description

La Selva Biological Station is located in the Atlantic lowlands of northeastern Costa Rica (10º26'N. 83º59'W, elevation range 37-150m). The 1,600ha site is located at the northwestern edge of 100,000ha of continuous forest that is comprised of a national park, national forests and private reserves (Clark et al. 2013). Classified as a tropical wet forest, the average daytime temperatures range from 24.7 to 27.1ºC. La Selva receives 3824mm of rainfall annually, with slightly lower rainfall occurring from January to April (McDade et al 1994).

One of the most extensively studied rainforest sites in the tropics, La Selva has 18-0.5ha forest inventory plots measured annually since 1997 (Figure 1). The plots are located within Old La Selva, which is bounded to the west by the Sarapiquí Annex and to the south by Braulio Carrillo National Park. These plots follow the ANPP (Aboveground NPP) measurement methodology, developed based on Clark and Clark (2001), and Huston and Wolverton (2009). The repeat plots sample old growth forest on the three different site conditions that dominate La Selva, with 6 plots on each (younger oxisol terrace, older oxisol plateau, older oxisol slope). Following the CARBONO description, all 18 plots were combined to one dataset representing La Selva old growth rainforest. For more on plot location and sampling design, see Clark and Clark 2000 or the CARBONO website (http://www.ots.ac.cr/carbonoproject). For an in-depth explanation of ANPP methodology, see Clark et al. (2013).

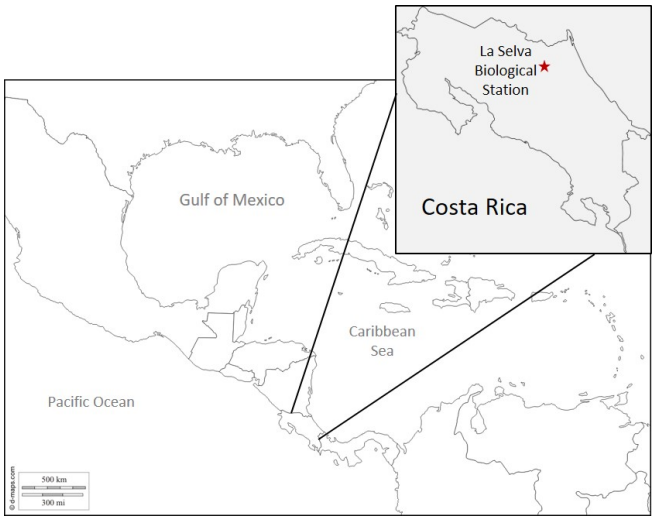

Figure 1 *The map indicates the study location, old growth forest in La Selva Biological Station, Costa Rica.*

FORMIND Model Description

For this study, we used the forest gap model FORMIND (Fischer et al., 2016). It is an individual- and process-based model designed especially for tropical forests considering the complex age- and size structure. With this model it is possible to investigate different forest attributes (e.g. biomass, leaf area, productivity) on user-defined spatial and temporal scales. The main processes in the model are the establishment of young trees, tree mortality, tree growth, and competition for light and space. As with the classic individual-based gap models, seeding, mortality and treefall are stochastic processes that through time lead to a mixed age, mixed species forest that reaches a stable equilibrium.

The biomass growth of each tree is determined on the basis of a carbon balance, which includes photosynthesis and respiration. Aboveground biomass B_{tree} [Mg] of a tree is calculated in relation to its stem diameter D [m] and height H_{tree} [m] by:

$$B_{tree} = \frac{\pi}{4} \cdot D^2 \cdot H_{tree} \cdot f \cdot \rho/\sigma \qquad (1)$$

whereby the calculation simply represents the volume of the tree stem (according to its geometry) multiplied by three factors, which describe the biomass content more concisely (Fischer et al. 2016). The form factor f [-] accounts for deviations of the stem from a cylindrical shape. The parameter ρ [Mg/m^3] is the wood density and the parameter σ [-] represents the fraction of total aboveground biomass attributed to the stem. Tree height H_{tree} [m] of a tree relates to its stem diameter D [m] by:

$$H_{tree} = h_0 \cdot D^{h_1} \qquad (2)$$

where h_0 and h_1 are species-specific parameters. The sum of the biomass of all trees within a certain area gives the biomass of a forest stand.

In FORMIND, tree growth is determined by a closed biomass balance, which is calculated for each tree, depending on its photosynthesis and respiration (Fischer et al. 2016):

$$\Delta B = \left(1 - r_g\right) \cdot \left(P_{tree} - R_m\right) \quad (3)$$

where r_g is a factor for growth respiration and R_m, the maintenance respiration. The photosynthesis P_{tree} of each tree is calculated depending on the shading and its geometry (Fischer et al. 2016) as:

$$P_{tree} = \frac{p_{max}}{k} \cdot \ln \frac{\alpha \cdot k \cdot I_{ind} + p_{max} \cdot (1-m)}{\alpha \cdot k \cdot I_{ind} \cdot e^{-k \cdot LAI} + p_{max} \cdot (1-m)} \quad (4)$$

where α is the quantum efficiency, also known as the initial slope of the light response curve, and p_{max} is the maximum leaf gross photosynthetic rate. The light extinction coefficient is k, m represents the transmission coefficient, and I_{ind} denotes the available incoming irradiance on top of the tree. The sum of P_{tree} for all trees gives GPP of the forest stand.

Finally, the LAI [m^2/m^2] can be calculated per tree as the one-sided leaf area per unit of crown projection area (i.e. the individual's leaf area index). This individual tree LAI relates functionally to its stem diameter D [cm] by:

$$LAI = l_0 \cdot D^{l_1} \quad (5)$$

where l_0 and l_1 are type-specific parameters (Fischer et al 2016).

The simulated forest area is divided into 20x20m patches according to the typical size of tree fall gaps. However, because these traits are calculated on an individual-tree basis, the 20m patches can be downscaled or upscaled according to the desired study area. Tree species with similar traits were grouped into plant functional types (PFT) according to physiological attributes such as maximum attainable height and light requirements (Fischer et al., 2018). A detailed description of the model can be found in Fischer et al. (2016). For this study, we parameterized FORMIND for the La Selva old growth forest, amalgamating plot data collected across the three dominant site conditions mentioned in the previous section. It is important to note that not all FORMIND model parameters could be derived from the available CARBONO dataset and from the literature. Where La Selva-specific data was not available, general parameters for rainforests for this region (Barro Colorado Island for example) were used (see Appendix B). A general FORMIND model description and the species grouping for La Selva can be found in Appendix A. A full listing of model parameters, both calculated from CARBONO and found in literature, as well as calibration metrics can be found in Appendix B.

Model Parameterization and Species Grouping

The forest inventory 18-plot dataset representing the old growth forest in La Selva, measured from 1997 through 2012 was downloaded from the CARBONO website. This dataset included species (where known) and DBH for each individual tree within the plot, measured annually. Maximum tree height per species was estimated from separate CARBONO data that included tree heights per some focal species (but was not included in the inventory plot dataset; Clark and Clark (1992, 2001), Dubayah et al. (2010), and King and Clark (2011). We calculated FORMIND parameters from maximum diameter growth increments per species and maximum DBH from years 1997 to 2005 and 2005 to 2012. Based on maximum DBH and diameter growth increment as calculated from the CARBONO dataset, the 190 species were grouped into six plant functional types (PFTs). A listing of this grouping can be found in Appendix A (*see:* Table A-3). For each of the six PFTs, we then calculated (based on CARBONO dataset) the following variables: stem counts, aboveground biomass, average diameter growth increment and mortality. A list of species group parameters can be found in Table 1 below.

Table 1 *A listing of size and light requirement parameters used to group species into plant functional types (PFTs) in the Costa Rican FORMIND Model.*

Size Class	Light Class	PFT	max DBH (mm)	max DBH growth (mm/yr)	max Height (m)	Field-estimated Biomass (Mg/ha)
Canopy Emergent	Shade Tolerant (ST)	1	>290	<5	48	49.32
	Shade Intermediate (INT)	2	>290	5-12	45	125.03
	Shade Intolerant (SI)	3	>290	>12	30	9.13
Sub-Canopy	ST	4	180-290	<5	20	14.375
	INT	5	180-291	5-12	15	1.17
Understory	ST	6	<180	<5	10	4.1

Model Calibration

When the model parameters were calculated, and entered into the FORMIND parameter file, simulations were run to calibrate some unknown parameter values (see above section). We performed a manual calibration to optimize a subsequent auto-calibration. The manual calibration was accomplished by running the model 250 times, systematically changing a few unknown parameters in small increments to achieve the best simulation of the study site forest (*see:* Lehmann and Huth 2015). Seed production and establishment of seedlings were high priority calibration variables, as there was little information in the literature and we relied on general values for the tropics. In addition, mortality and light response curves were also optimized.

When the manual calibration for each of these variables determined ideal ranges for each PFT, remaining unknown parameters were numerically calibrated (e.g., global number of seeds) with a calibration process by comparing the aboveground biomass, species composition, and tree density of a simulated mature forest with field data from the study region following Lehmann and Huth (2015). The parameterization was then verified by comparison of stem numbers per diameter size classes, aboveground biomass, basal area and other structural variables (see Figure 3 in *Results*).

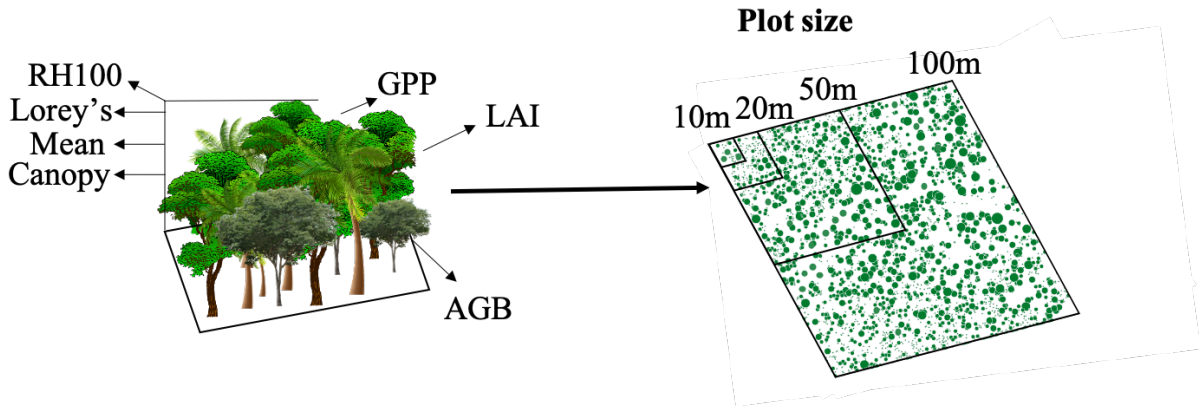

Figure 2 This conceptual diagram represents the resolution scale differences at which we conducted our analysis of four definitions of height (RH100, Canopy, Lorey's and Mean) with aboveground biomass (AGB), leaf area index (LAI) and gross primary production (GPP).

Simulation Settings

We analyzed forest succession over 1,000 years, starting with bare ground conditions, in order to ensure that the simulation encompassed the full life history of the rainforest. To assess the full structural variability in the forest model, we simulated forest stands with a size of 16 hectares. First, for a comparison of the model output with field data, we calculated the mean of simulated forest attributes over the last 300-1,000 years, based on the assumption that the forest is in the equilibrium state for this entire period. In particular, we included aboveground biomass, basal area, and stem numbers for trees with a DBH greater than 10cm. Second, we analyzed the relationship between Lorey's height and AGB, LAI and GPP at four different resolutions (10m, 20m, 50m, 100m). All simulated forest stands between simulation years 300 to 1000 were aggregated into one large dataset. The dataset was then divided into 10m plots, 20m plots, 50m plots and 100m plots in order to collect the height variables, and the AGB, LAI and GPP at each of the resolutions for comparison. The AGB, LAI and GPP were recorded per varied plot size (e.g. 10m, 20m, 50m and 100m) and then scaled to a per hectare measurement. In order to avoid biasing our comparisons with uneven numbers of data points between each of the resolutions, 8,000 random plot data points were collected for each of the variables at each resolution. Similar methodologies have been undertaken by Mascaro et al (2012) and Knapp et al (2018).

For the forest height calculation, we investigated four different common height definitions, including mean tree height (Mean), maximum height as also derived by lidar (RH100), canopy height (Canopy) and Lorey's height. The mean tree height is the average of all tree heights (with DBH>10cm) within the plot size (10m to 100m). The maximum height is the height of the tallest tree within the plot. Canopy height is the mean of all tree heights within the canopy, as defined by Kohler and Huth (2010). Lorey's height is the basal-area-weighted average tree height of trees in the plot (Lorey 1878).

Results

Forest Model vs. Field data

To test the parameterization for La Selva rainforest, we compared simulated basal area, aboveground biomass and stem numbers to forest inventory data, scaled to one hectare. Forest height was also compared to Kellner et al's (2009) findings (see Appendix B). Comparisons were made on the level of PFT. We found that when the forest reaches equilibrium after year 200, large intermediate trees (PFT 2) are dominant, followed by large shade tolerant trees (PFT 1). Shade intolerant (PFT 3), sub-canopy shade tolerant (PFT 4), sub-canopy intermediate (PFT 5), and understory shade tolerant (PFT 6) trees together make up only about 5% of the total forest aboveground biomass.

There is an initial large increase of biomass with the colonization by pioneer shade intolerant trees (PFT 3, cf. Fig. 3c). Shade intermediate trees (PFT 2) quickly compete with shade intolerant trees, followed by shade tolerant canopy (PFT 1), shade tolerant sub canopy trees (PFT 4), and intermediate sub canopy trees (PFT 5). As the shade tolerant (PFT 1) canopy, shade tolerant sub canopy (PFT 4) and intermediate sub-canopy (PFT 5) trees colonize the understory (*ca.* year 40), shade intolerant trees reach maturity and quickly decline in numbers and biomass.

By year 200 of the simulated forest life history, the forest reaches a stable equilibrium (Fig. 3a, 3c). Intermediate canopy and emergent trees make up the dominant proportion of biomass (61.6%), followed by shade tolerant canopy and emergent trees (24.3%). Shade tolerant sub canopy trees (PFT4) account for about 7.0% of the total aboveground biomass. The remaining plant functional type groups (PFT 3, PFT 5 and PFT 6) are responsible for only a

small percentage of the aboveground biomass (8.4%). In comparing field data to the simulation, aboveground biomass for the simulated forest was ca. 200 Megagrams of organic try matter per ha (Mg_{ODM}/ha), which was 2.3% lower than observed in the field data (204.61 Mg/ha) (Fig. 3d). The model slightly underestimates aboveground biomass for PFT 1, and overestimates for PFT 4 (+/- 1% for each).

The total basal area of the forest was slightly underestimated by FORMIND, with values of 20.5 m^2/ha compared to 21.5 m^2/ha measured in the actual forest (Fig. 3b). Also underestimated was basal area of PFT2, which had the largest biomass of all the PFTs, and accounted for most of the total difference (11.3 m^2/ha simulated, compared with 12.3 m^2/ha field measured). The simulated basal area for PFT4, was the only overestimation by the model; it accounted for 14.1% of the total simulated basal area, as compared to 12.3% of the total La Selva measured basal area. Basal area of PFTs 1 and 3 were exactly the same when comparing simulated and measured values, while PFTs 5 and 6 were underestimated by the model with differences of 0.33 m^2/ha and 0.16 m^2/ha, respectively. A detailed evaluation of stem number distributions can be found in Appendix B.

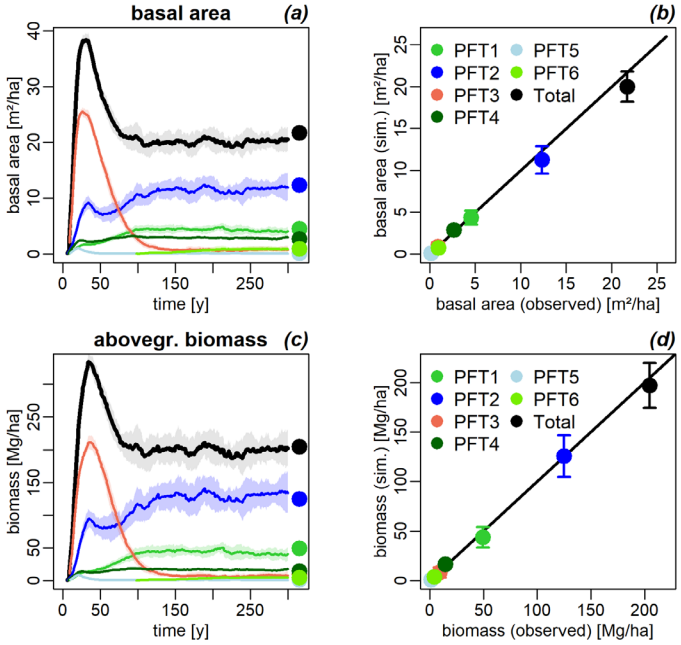

Figure 3 *Left column from top to bottom*: Time series showing basal area in m^2/ha (*a*) and aboveground biomass in Mg/ha (*c*) from a bare ground state at year 0 to 300 years. After 300 years, the forest is in a stable equilibrium and appear similar to years 200-300. The dots at the far right of the figures show the variables as calculated from the field data set, with colors corresponding to PFT number and color groups to light requirements (i.e. greens are shade tolerant, blues shade intermediate, red shade intolerant and total in black). *Right column from top to bottom:* 1:1 comparison between field data calculations (x-axis) and simulation values for late-successional phase of the simulated forest for basal area in m^2/ha (b) and aboveground biomass in Mg/ha (*d*).

Forest Height vs. Aboveground Biomass

In the forest structure analysis comparing four measures of height to aboveground biomass averaged at four different plot resolutions, we found that the relationship was weaker at larger scales, but the strength of the relationship also depends on the height definition. The comparison of maximum height (RH100) and canopy height to AGB at 10mx10m plot resolution both had the overall strongest relationship (*see* Appendix C). With each of the height definitions used in our study, the relationship with AGB was best described using a power-law function. For the relationship between biomass and height on the 10m scale, the R^2 values for

mean height, RH100, canopy height and Lorey's height was found to be 0.6, 0.91, 0.91 and 0.83, respectively. Detailed results for the RH100, canopy height and mean height correlations with AGB are found in Appendix C.

When Lorey's height is compared to AGB at 20 x 20m resolution (Figure 4b), the predictive capability of the AGB-height relationship decreases to an R^2 of 0.70. This decreasing trend continues at coarser resolutions: R^2 decreases at the 50m resolution to 0.59, and 0.54 at 100m resolution (Fig. *4c*, *4d*). Conversely, the RMSE of the Lorey's height-AGB relationship improves drastically as the resolution coarsens, from 135.3 Mg/ha at 10m resolution, to 15.9 Mg/ha at 100m resolution. This inverse relationship between R^2 and RMSE is explained by the behavior of the plots in Figure 4 (*a-d*). At the 10m resolution (Fig. *4a*), the points spread throughout the entire height range of the equation that is produced by the best fit line. However, the distances of the points to the best fit line (RMSE) is overall much larger than the distances of the points to the 100m resolution best fit line (Fig. *4d*), which does not extend over the full range of Lorey's height.

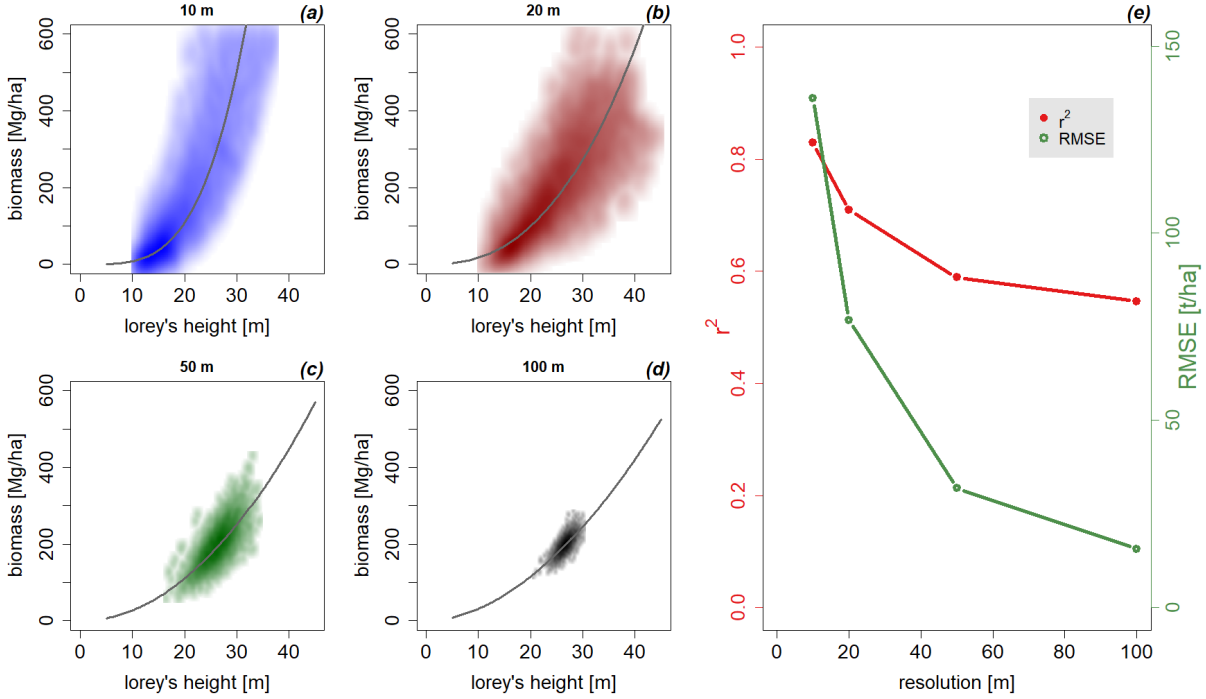

Figure 4 At left: *The four plots display the relationship between Lorey's height (m) and aboveground biomass (Mg_{odm}/ha) at plot scales of* (a) *10x10m (100m^2 = 0.01ha) in blue, (b) 20x20m (400m^2 = 0.04ha) in red, (c) 50x50m (2500m^2 = 0.25ha) in green, and (d) 100x100m (10000m^2 = 1.0ha) in black. Note: For the purposes of visual comparison, the scale of figures (a) through (d) was kept consistent. Nonetheless, the datasets in figures (a) and (b) are not truncated. Above, (e): The figure compares the Root Mean Squared error at each plot resolution is (green) and the R^2 value at each plot resolution; both were calculated from the best-fit lines for each dataset shown on the left.*

Forest Height vs. Leaf Area Index (LAI)

We compared how LAI varies among the four measures of canopy height at different plot scales (Fig. 5). Lorey's height related best to LAI at the 10m resolution (R^2: 0.75), with decreasing R^2 values as the plot size increased to 100m (0.27). As with AGB, the R^2 values decrease with increasing resolution coarseness, however, with LAI, the strength of the relationship decreases more rapidly; indeed, at 20m plot resolution the R^2 value is 0.52 and the relationship between LAI and Lorey's height at 50m and 100m resolutions cannot be considered meaningful (0.35 and 0.27, respectively).

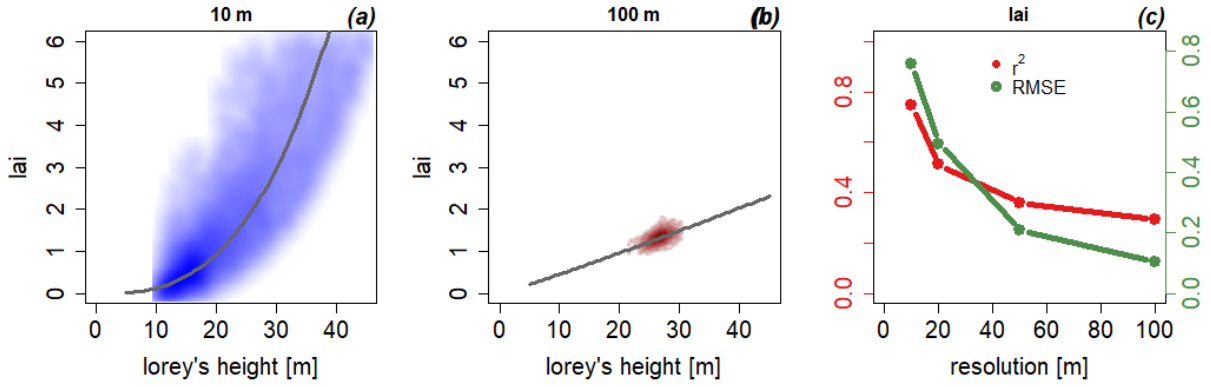

Figure 5. *Plots showing the relationship of Lorey's height to Leaf Area Index (LAI) for the simulated forest at the 10m (a) and 100m (b) scales, including best fit lines in black. RMSE and R^2 at all four resolutions are shown in red and green in plot (c). Note: For the purposes of visual comparison, the scale of figure (a) was kept consistent with that of (b). However, the dataset in figure (a) is not truncated.*

When Lorey's height is compared to LAI, the RMSE also decreases with coarsening resolution, from 0.8 to 0.1. LAI is commonly defined as the maximum projected leaf area per unit ground surface. This inherently includes all leaf material from the top of the canopy downward through the vertical leaf profile, so it necessitates a height measure that is reflective of the top height of the plot canopy, which is a possible source of error with respect to fit of the relationship. Mixed heterogeneous forests like that of La Selva have a large variation in LAI values when measured at fine scales; variation that would be averaged out at large plot scales. An in-depth comparison of each of the different height measurements to LAI at each plot resolution is found in Appendix D.

Forest Height vs Gross Primary Productivity (GPP)

The relationship between simulated height and gross primary productivity (GPP) is also best described using a power law function, as shown in Figure 6. Ryan et al (1994) measured GPP in La Selva to be around 50 Mg/ha/year, which is in the same order as our simulated GPP values (40 Mg/ha/year). The correlation of Lorey's height to GPP was most clear at the highest resolution with R^2 values of 0.78 at 10m resolution and 0.61 at 20m resolution. At the 50m

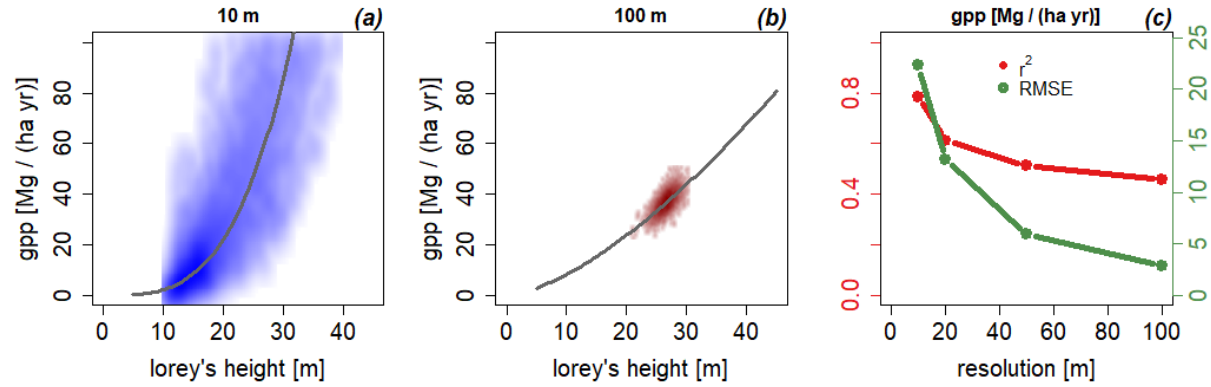

Figure 6 *Plots showing the relationship of Lorey's height to yearly Gross Primary Production (GPP) in tonnes biomass per hectare and year for the simulated forest at the 10m (a) and 100m (b) scales, including best fit lines in black. RMSE and R^2 at all four resolutions are shown in red and green in plot (c). Note: For the purposes of visual comparison, the scale of figure (a) was kept consistent with that of (b). However, the dataset in figure (a) is not truncated.*

resolution however, the correlation was weaker and had an R^2 of 0.5, and was most weak when measured at the 100m resolution ($R^2 = 0.43$). As with the ABG and LAI comparisons, the RMSE of the Lorey's height to GPP relationship decrease with increasing plot size. At the 10m plot resolution, RMSE is 20.05 Mg/ha but decreases by almost half for each successive plot size, from 12.07 Mg/ha at 20m plot resolution, to 5.17 Mg/ha at 50m plot resolution and 2.63 Mg/ha at 100m plot resolution. The comparisons of each of the different height measurements to GPP at each plot resolution is found in Appendix E.

Error

The root mean-squared error (RMSE) was calculated for each correlation, at all scales and for each height definition. As shown in Appendix F, in all correlations RMSE was highest at 10m resolution and decreased as the resolution coarsened to 100m. When the RMSE and R^2 values were plotted for each resolution, the high RMSE values declined sharply between 10m and 20m resolution, whereas the R^2 values decreased less sharply (*see Appendix C, D, E and F figures*). These differences in values between resolutions and the directionality of their trends suggest that though the data at the smallest resolutions is the noisiest, their R^2 high value indicates the ranges of points fit best the power equation.

Discussion

Overall, our study shows that the strength of the height to AGB, LAI and GPP relationships are the best at the smaller spatial scales, however this comes with an increase in error. At coarser scales the error becomes smaller, but the relationship between the forest variables become less precise (Figure 1a). Using FORMIND model simulations helped to quantify this trade-off between accuracy and precision across the plot resolutions. Toward informing the initial research question of "*How does the crucial relationship between canopy height metrics and forest stand biomass (AGB), leaf area index (LAI) and gross primary productivity (GPP) change at different spatial resolutions?",* relating height variables to this study's focal productivity variables is best at the scale of a very small plot. Given that the average width of the crown of a canopy emergent tree in La Selva rainforests typically exceeds 10m in diameter (King and Clark 2011, Obrien et al 1995) and the 10m plots size revealed the largest RMSE across each of the compared variables, a plot size of 20m affords the most reliable and robust comparison.

Data from La Selva forest inventory plots was used to successfully create a parameterization of the FORMIND model. This parameterization is the first for this specific type of fine-scaled individual- and process-based gap model for La Selva biological station that includes fine-scale structural realism. The dataset used to parameterize FORMIND for La Selva is exceptional compared to many tropical rainforest datasets in terms of longevity and replication. Only a handful of other tropical rainforest sites (e.g. Barro Colorado Island, Panama and Paracou, French Guiana) within this region have a similar study area inventoried and are repeated over decades. Given the robustness of the inventory data, *in situ* measurement error is not likely the source of any significant model parameterization uncertainty. It is more likely that the main source of uncertainty with respect to the discrepancies found between the simulated forest and the inventory dataset is due to uncertainties in grouping the La Selva species into plant functional types, and due to prominence of palms and other growth forms in general that are not simulated by FORMIND.

Similarly, using the maximum diameter growth increment could result in a few placement errors. For example, a rarely occurring shade tolerant tree species that is released from canopy suppression might have a large maximum diameter growth increment for a short period of time that more closely resembles a shade intolerant pioneer species and would result

in an uncharacteristically high maximum diameter growth increment for that particular species over the timespan that was used to calculate it. Either of these scenarios could have resulted in a few of the less common tree species being placed into incorrect PFTs. Ideally, the modeled forest should be compared to a validation dataset in order to more thoroughly investigate the causes of uncertainty.

As presented in Fischer et al. 2016, and also in Rodig et al 2018, the FORMIND model has been shown to be a useful tool in studies that aim to understand relationships between numerous forest structure variables and other measurable ecosystem functions, including forest biomass and forest productivity. We used the Costa Rican FORMIND model to investigate how four definitions of tree height vary with AGB, LAI and GPP at plot resolutions. As was shown by the simulation results, height is relatable to AGB, LAI and GPP using a power law. In Costa Rican rainforest, a taller forest has higher aboveground biomass, more leaves and thus a higher LAI, and is overall more productive then smaller stands.

Though the relationship varied with resolution, the simulated LAI was comparable to values found by Clark et al (2008) in their study directly measuring LAI across numerous plant functional groups in La Selva Biological Station. Their study found a total LAI of 6 for old growth forest, however the total included lianas, palms, herbaceous climbers, herbs, ferns and epiphytes. As FORMIND includes only trees greater than 10cm DBH, it compares well to the mean LAI for trees only, which was measured to be 3.29 by Clark et al (2008), and 3.30-4.79 (median) by Loedscher et al (2003). One study, by Tang et al in 2012, which created vertical LAI profiles from canopy waveform lidar (LVIS) and a radiative transfer model (GORT), found slightly higher forest LAI values. When subtracting out the non-tree forest constituents, the LAI in this study is consistent within a reasonable range of all three existing studies.

The values for GPP as calculated by the model output are also congruent with the literature. Loescher et al (2003) calculated Gross Ecosystem Productivity (GEP) values between 28.4 and 30.6 from tower measurements taken in 1998 and 1999, respectively. Luyssaert et al 2007 reported a GPP value of 35.5 ±1.60 $tCha^{-1}yr^{-1}$ for tropical humid evergreen forest in a study comparing GPP across forest types.

This study highlights the capability of individual based modeling as the appropriate model platform to investigate forest structure and scale directly. Our study did not attempt to define the 'best' height definition to use because different height definitions are widely accepted among forest ecologists and across the different remote sensing platforms (*see* Appendices). Instead, we sought to understand how fine-scale characterization of height is more accurate than at coarser scales. While fine scale measurements tend to add some noise, overall they provided a clearer picture of height, with less error. In addition, canopy height, RH100 and then Lorey's height tended to relate best to aboveground biomass, leaf area index and gross primary productivity, respectively.

Advances in remote sensing data processing have facilitated calibration of variables of interest with forest inventory plot datasets for scaling to landscape-level estimations of aboveground biomass and carbon flux (Baccini et al. 2012; Saatchi et al. 2011a; Morel et al. 2011). Additionally, many of the recent change maps of AGB and carbon flux rely on classification and calibration of remotely sensed datasets with measured or leveraged fine-scale forest structure ground truth data points (Asner et al. 2009; Hansen et al. 2013; Hansen et al. 2016; Hudak et al. 2012). Remote sensing approaches are among the solutions for a large-scale systematic vegetation monitoring, though they are often limited by sensor footprint. In these applications typically in situ field inventory measurements are used to calibrate the remote sensing dataset, but due to the lack of data temporal coverage and long-term monitoring plots, constitute only a snapshot of the forest and are constrained to imagery collected during the same time period or risk introduction of additional uncertainty.

With the advancement of super-computing and cloud-based processors, scaling of high-resolution datasets across landscapes has never been easier. It is therefore crucial to gain

knowledge of how to minimize error and uncertainty when applying high resolution datasets across landscapes. Particularly in the tropics, where aboveground biomass is based largely on broad allometric relationships calculated from stem diameters and wood density (Chave et al. 2014; Chave et al. 2005; Chave et al. 2004), error estimates are often higher than in temperate forests, for which allometric equations are more robust (Malhi et al. 1999; Ketterings et al. 2001; Chave et al. 2004). This study also highlights the importance of realizing and accounting for the differences of measuring forest structure using top-down versus bottom-up approaches. In Meyer et al.'s 2013 study using repeated LiDAR (LVIS and DRL) to detect tropical forest biomass dynamics across the same La Selva study site, they found a reduction of error and uncertainty (RMSE) as resolution coarsened.

Tree height is an important forest structure variable that can be both directly measured *in situ* and obtained remotely as canopy height, using various methods with lidar and radar interferometry (Popescu 2007; Hyde et al. 2007; Lefsky et al. 2005; Zheng et al, 2004; Dubayah et al. 1997). Either directly measured from the ground up during forest inventories, or calculated through allometric equations, tree height has become widely used as a predictor of aboveground biomass, as well as other indirectly measured forest variables. This study also highlights the importance of realizing and accounting for the differences of measuring forest structure using top-down versus bottom-up approaches.

Canopy height, in addition to other vertical canopy variables relating top of the canopy to the ground, have been used to characterize vertical structure across numerous forest types from the top down (Drake et al. 2002; Dubayah et al. 1997, 2000; Blair et al. 1999; Lefsky et al. 1999; Weishampel et al. 1996). As noted by Kohler and Huth (2010), the height of the canopy in forests is a key variable which can be obtained using air- or space-borne remote sensing techniques such as radar interferometry or lidar. The wide variety of sensors has greatly increased resolution over the past decades. For example, most lidar footprints range in diameter, including LVIS (25m), UAVSAR (6m in 100kmx20km transects), GEDI (20m) and ICESAT (60m) aboard GLAS. However, recently some sensors have even higher resolution (e.g. G-LiHT with its <1m resolution; Cook et al. 2013). Various studies set in tropical ecosystems have successfully used remote sensing to characterize forest structure variables (e.g. Dubayah et al., 2010, Potter et al., 2009; Frolking et al., 2009, Garrigues et al., 2008) and by application of plot data to infer regional estimates of AGB forest characterization (e.g. Malhi et al., 2006; Saatchi et al., 2007).

According to Drake et al. (2002), because many remote sensing studies estimate forest biomass using empirical correlations of energy and different wavelengths, the approach (and sensors) are sensitive to biomass changes in relatively young forests, but tend to saturate and become less predictable in older growth and heterogeneous forests. In Meyer et al.'s 2013 study using repeated lidar (LVIS and DRL) to detect tropical forest biomass dynamics across the same La Selva study site, they found a reduction of error and uncertainty (RMSE) as resolution coarsened from 10m x 10m plots to 100m x 100m plots. This difference in findings can be accounted for in two fundamental ways. First, Meyer et al used a pixel based approach with a 1m fixed resolution CHM, which was averaged to the target pixel size from 0.4ha to 10ha. Our study uses height values based on individual trees within a plot, whereby the plot heights were obtained according to which trees grew in a given plot during a given year, with the size of the plot varying from 0.01ha to 1ha. Essentially, the resolution of our CHM was variable and congruous to plot resolution. Second, our study is more theoretical. We used a sampling approach to construct our analyses so that an equal number of points was plotted regardless of the resolution. This was done to ensure that our analysis was not subjected to sample bias in comparing plots with an unequal number of points between resolutions influencing the fit of the relationship (R^2) or the error (RMSE).

Conclusion

Individual-based models like FORMIND can be used to further the capabilities of remote sensing through modeling applications aimed at drawing empirical relationships at scales that are too fine to be measured with sensors, but that could be scaled up to be applied in remote sensing studies. The results of our study can shed light on why forest height cannot accurately predict aboveground biomass at coarser scales when measuring from the ground up: we show that regardless of how height is defined, the empirical relationship breaks down when trees are scaled to 60-meter and 100-meter plots. Because lidar and radar interferometry are well suited to determine forest height from the top down, there exists a natural synergism with individual-based models like FORMIND. However, because of the difference in methodology with which high resolution models and remote sensing methods obtain height metrics, it is important to consider and resolve resolution where possible. When the height is based on per tree values, the accuracy of prediction of AGB, LAI and GPP is higher, but there is a trade off with precision. With respect to high resolution modeling, the aim should therefore be to first define the intended error margins, then scale the resolution of the study accordingly.

References

Armstrong, A., Fischer, R., Huth, A., Shugart, H. and Fatoyinbo, T., 2018. Simulating forest dynamics of lowland rainforests in Eastern Madagascar. Forests, 9(4), p.214.

Asner, G.P., Hughes, R.F., Varga, T.A., Knapp, D.E. and Kennedy-Bowdoin, T., 2009. Environmental and biotic controls over aboveground biomass throughout a tropical rain forest. Ecosystems, 12(2), pp.261-278.

Baccini, A.G.S.J., Goetz, S.J., Walker, W.S., Laporte, N.T., Sun, M., Sulla-Menashe, D., Hackler, J., Beck, P.S.A., Dubayah, R., Friedl, M.A. and Samanta, S., 2012. Estimated carbon dioxide emissions from tropical deforestation improved by carbon-density maps. Nature climate change, 2(3), p.182.

Blair, J.B., Rabine, D.L. and Hofton, M.A., 1999. The Laser Vegetation Imaging Sensor: a medium-altitude, digitisation-only, airborne laser altimeter for mapping vegetation and topography. ISPRS Journal of Photogrammetry and Remote Sensing, 54(2), pp.115-122.

Botkin, D.B., Janak, J.F. and Wallis, J.R., 1972. Some ecological consequences of a computer model of forest growth. The Journal of Ecology, pp.849-872.

Bugmann, H., 2001. A review of forest gap models. Climatic Change, 51(3-4), pp.259-305.
CARBONO Project (1 December 2014) http://www.ots.ac.cr/carbonoproject

Chave, J., Condit, R., Lao, S., Caspersen, J.P., Foster, R.B. and Hubbell, S.P., 2003. Spatial and temporal variation of biomass in a tropical forest: results from a large census plot in Panama. Journal of Ecology, 91(2), pp.240-252.

Chave, J., Condit, R., Aguilar, S., Hernandez, A., Lao, S. and Perez, R., 2004. Error propagation and scaling for tropical forest biomass estimates. Philosophical Transactions of the Royal Society of London B: Biological Sciences, 359(1443), pp.409-420.

Chave, J., Andalo, C., Brown, S., Cairns, M.A., Chambers, J.Q., Eamus, D., Fölster, H., Fromard, F., Higuchi, N., Kira, T. and Lescure, J.P., 2005. Tree allometry and improved estimation of carbon stocks and balance in tropical forests. Oecologia, 145(1), pp.87-99.

Chave, J., Olivier, J., Bongers, F., Châtelet, P., Forget, P.M., van der Meer, P., Norden, N., Riéra, B. and Charles-Dominique, P., 2008. Above-ground biomass and productivity in a rain forest of eastern South America. Journal of Tropical Ecology, 24(4), pp.355-366.

Chave, J., 2013. The problem of pattern and scale in ecology: what have we learned in 20 years? Ecology Letters, 16(s1), pp.4-16.

Chave, J., Réjou-Méchain, M., Búrquez, A., Chidumayo, E., Colgan, M.S., Delitti, W.B., Duque, A., Eid, T., Fearnside, P.M., Goodman, R.C. and Henry, M., 2014. Improved allometric models to estimate the aboveground biomass of tropical trees. Global change biology, 20(10), pp.3177-3190.

Clark, D.A. and Clark, D.B., 1992. Life history diversity of canopy and emergent trees in a neotropical rain forest. Ecological monographs, 62(3), pp.315-344.

Clark, D.B. and Clark, D.A., 2000. Landscape-scale variation in forest structure and biomass in a tropical rain forest. Forest ecology and management, 137(1), pp.185-198.

Clark, D.A. and Clark, D.B., 2001. Getting to the canopy: tree height growth in a neotropical rain forest. Ecology, 82(5), pp.1460-1472.

Clark, D. B., and D. A. Clark. 2006. Tree growth, mortality, physical and microsite in an old-growth lowland tropical rain forest. Ecology, 87, 2132, http://www.esapu bs.org /arc hive/e col/E087/132de fault.htm.

Clark, D.B., Olivas, P.C., Oberbauer, S.F., Clark, D.A. and Ryan, M.G., 2008. First direct landscape-scale measurement of tropical rain forest Leaf Area Index, a key driver of global primary productivity. Ecology letters, 11(2), pp.163-172.

Clark, D.A., Clark, D.B. and Oberbauer, S.F., 2013. Field-quantified responses of tropical rainforest aboveground productivity to increasing CO2 and climatic stress, 1997–2009. Journal of Geophysical Research: Biogeosciences, 118(2), pp.783-794.

Clark, D.B., Hurtado, J. and Saatchi, S.S., 2015. Tropical rain forest structure, tree growth and dynamics along a 2700-m elevational transect in Costa Rica. PloS one, 10(4), p.e0122905.

Cook, B. D., L. W. Corp, R. F. Nelson, E. M. Middleton, D. C. Morton, J. T. McCorkel, J. G. Masek, K. J. Ranson, V. Ly, and P. M. Montesano. 2013. NASA Goddard's Lidar, Hyperspectral and Thermal (G-LiHT) airborne imager. Remote Sensing 5:4045-4066, doi:10.3390/rs5084045

Dixon, R.K., Brown, S., Houghton, R.E.A., Solomon, A.M., Trexler, M.C. and Wisniewski, J., 1994. Carbon pools and flux of global forest ecosystems. Science(Washington), 263(5144), pp.185-189.

Drake, J.B., Dubayah, R.O., Clark, D.B., Knox, R.G., Blair, J.B., Hofton, M.A., Chazdon, R.L., Weishampel, J.F. and Prince, S., 2002. Estimation of tropical forest structural characteristics using large-footprint lidar. Remote Sensing of Environment, 79(2), pp.305-319.

Drake, J.B., Knox, R.G., Dubayah, R.O., Clark, D.B., Condit, R., Blair, J.B. and Hofton, M., 2003. Above-ground biomass estimation in closed canopy neotropical forests using lidar remote sensing: Factors affecting the generality of relationships. Global ecology and biogeography, 12(2), pp.147-159.

Dubayah, R., Prince, S., JaJa, J., Blair, J.B., Bufton, J.L., Knox, R., Luthcke, S.B., Clarke, D.B. and Weishampel, J., 1997. The vegetation canopy lidar mission. Land satellite information in the next decade II: sources and applications.

Dubayah, R., Knox, R., Hofton, M., Blair, J.B. and Drake, J., 2000. Land surface characterization using lidar remote sensing. Spatial information for land use management, pp.25-38.

Dubayah, R.O., Sheldon, S.L., Clark, D.B., Hofton, M.A., Blair, J.B., Hurtt, G.C. and Chazdon, R.L., 2010. Estimation of tropical forest height and biomass dynamics using lidar remote sensing at La Selva, Costa Rica. Journal of Geophysical Research: Biogeosciences, 115(G2).

Fischer, R.; Armstrong, A.H.; Shugart, H.; Huth, A. 2014. Simulating the impacts of reduced rainfall on carbon stocks and net ecosystem exchange in a tropical forest. Environmental Modelling and Software, 52, 200-206.

Fischer, R., Bohn, F., de Paula, M.D., Dislich, C., Groeneveld, J., Gutiérrez, A.G., Kazmierczak, M., Knapp, N., Lehmann, S., Paulick, S. and Pütz, S., 2016. Lessons learned from applying a forest gap model to understand ecosystem and carbon dynamics of complex tropical forests. Ecological Modelling, 326, pp.124-133.

Fischer, R., Rödig, E. and Huth, A., 2018. Consequences of a Reduced Number of Plant Functional Types for the Simulation of Forest Productivity. Forests, 9(8), p.460.

Frolking, S., Palace, M.W., Clark, D.B., Chambers, J.Q., Shugart, H.H. and Hurtt, G.C., 2009. Forest disturbance and recovery: A general review in the context of spaceborne remote sensing of impacts on aboveground biomass and canopy structure. Journal of Geophysical Research: Biogeosciences, 114(G2).

Garrigues, S., Lacaze, R., Baret, F.J.T.M., Morisette, J.T., Weiss, M., Nickeson, J.E., Fernandes, R., Plummer, S., Shabanov, N.V., Myneni, R.B. and Knyazikhin, Y., 2008. Validation and intercomparison of global Leaf Area Index products derived from remote sensing data. Journal of Geophysical Research: Biogeosciences, 113(G2).

Hansen, M.C., Potapov, P.V., Moore, R., Hancher, M., Turubanova, S.A.A., Tyukavina, A., Thau, D., Stehman, S.V., Goetz, S.J., Loveland, T.R. and Kommareddy, A., 2013. High-resolution global maps of 21st-century forest cover change. science, 342(6160), pp.850-853.

Hansen, M.C., Potapov, P.V., Goetz, S.J., Turubanova, S., Tyukavina, A., Krylov, A., Kommareddy, A. and Egorov, A., 2016. Mapping tree height distributions in Sub-Saharan Africa using Landsat 7 and 8 data. Remote Sensing of Environment, 185, pp.221-232.

Hudak, A.T., Strand, E.K., Vierling, L.A., Byrne, J.C., Eitel, J.U., Martinuzzi, S. and Falkowski, M.J., 2012. Quantifying aboveground forest carbon pools and fluxes from repeat LiDAR surveys. Remote Sensing of Environment, 123, pp.25-40.

Hurtt, G.C., Dubayah, R., Drake, J., Moorcroft, P.R., Pacala, S. and Fearon, M., 2004. Beyond potential vegetation: combining lidar remote sensing and a height-structured ecosystem model for improved estimates of carbon stocks and fluxes. Ecological Applications, 14(3), pp.873-883.

Hurtt, G.C., Fisk, J., Thomas, R.Q., Dubayah, R., Moorcroft, P.R. and Shugart, H.H., 2010. Linking models and data on vegetation structure. Journal of Geophysical Research: Biogeosciences, 115(G2).

Huston, M.A. and Wolverton, S., 2009. The global distribution of net primary production: resolving the paradox. Ecological monographs, 79(3), pp.343-377.

Huth, A., Drechsler, M. and Köhler, P., 2005. Using multicriteria decision analysis and a forest growth model to assess impacts of tree harvesting in Dipterocarp lowland rain forests. Forest Ecology and Management, 207(1-2), pp.215-232.

Hyde, P., Nelson, R., Kimes, D. and Levine, E., 2007. Exploring LiDAR–RaDAR synergy—predicting aboveground biomass in a southwestern ponderosa pine forest using LiDAR, SAR and InSAR. Remote Sensing of Environment, 106(1), pp.28-38.

Kellner, J.R., Clark, D.B. and Hubbell, S.P., 2009. Pervasive canopy dynamics produce short-term stability in a tropical rain forest landscape. Ecology Letters, 12(2), pp.155-164.

Ketterings, Q.M., Coe, R., van Noordwijk, M. and Palm, C.A., 2001. Reducing uncertainty in the use of allometric biomass equations for predicting above-ground tree biomass in mixed secondary forests. Forest Ecology and management, 146(1), pp.199-209.

King, D.A., 1996. Allometry and life history of tropical trees. Journal of tropical ecology, 12(1), pp.25-44.

King, D.A. and Clark, D.A., 2011. Allometry of emergent tree species from saplings to above-canopy adults in a Costa Rican rain forest. Journal of Tropical Ecology, 27(6), pp.573-579.

Köhler, P. and Huth, A., 1998. The effects of tree species grouping in tropical rainforest modelling: simulations with the individual-based model FORMIND. Ecological Modelling, 109(3), pp.301-321.

Köhler, P., Ditzer, T. and Huth, A., 2000. Concepts for the aggregation of tropical tree species into functional types and the application to Sabah's lowland rain forests. Journal of Tropical Ecology, 16(4), pp.591-602.

Köhler, P. and Huth, A., 2007. Impacts of recruitment limitation and canopy disturbance on tropical tree species richness. ecological modelling, 203(3-4), pp.511-517.

Köhler, P. and Huth, A., 2010. Towards ground-truthing of spaceborne estimates of above-ground life biomass and leaf area index in tropical rain forests. Biogeosciences, 7, pp.2531-2543.

Köhler, P., Chave, J., Riéra, B. and Huth, A., 2003. Simulating the long-term response of tropical wet forests to fragmentation. Ecosystems, 6(2), pp.0114-0128.

Knapp, N., Fischer, R. and Huth, A., 2018. Linking lidar and forest modeling to assess biomass estimation across scales and disturbance states. Remote Sensing of Environment, 205, pp.199-209.

Lefsky, M.A., Harding, D., Cohen, W.B., Parker, G. and Shugart, H.H., 1999. Surface lidar remote sensing of basal area and biomass in deciduous forests of eastern Maryland, USA. Remote Sensing of Environment, 67(1), pp.83-98.

Lefsky, M.A., Cohen, W.B., Parker, G.G. and Harding, D.J., 2002. Lidar remote sensing for ecosystem studies: Lidar, an emerging remote sensing technology that directly measures the three-dimensional distribution of plant canopies, can accurately estimate vegetation structural attributes and should be of particular interest to forest, landscape, and global ecologists. AIBS Bulletin, 52(1), pp.19-30.

Lefsky, M.A., Harding, D.J., Keller, M., Cohen, W.B., Carabajal, C.C., Del Bom Espirito-Santo, F., Hunter, M.O. and de Oliveira, R., 2005. Estimates of forest canopy height and aboveground biomass using ICESat. Geophysical research letters, 32(22).

Lehmann, S. and Huth, A., 2015. Fast calibration of a dynamic vegetation model with minimum observation data. Ecological modelling, 301, pp.98-105.

Loescher, H.W., Oberbauer, S.F., Gholz, H.L. and Clark, D.B., 2003. Environmental controls on net ecosystem-level carbon exchange and productivity in a Central American tropical wet forest. Global Change Biology, 9(3), pp.396-412.

Lorey, T., 1878. Die mittlere Bestandeshöhe. *translated: "The mean stock height*." Allgemeine Forst und Jagdzeitung/Journal of Forestry and Hunting. 54,149–155.

Luyssaert, S., Inglima, I., Jung, M., Richardson, A.D., Reichstein, M., Papale, D., Piao, S.L., Schulze, E.D., Wingate, L., Matteucci, G. and Aragao, L.E.O.C., 2007. CO2 balance of boreal, temperate, and tropical forests derived from a global database. Global change biology, 13(12), pp.2509-2537.

Malhi, Y.A., Baldocchi, D.D. and Jarvis, P.G., 1999. The carbon balance of tropical, temperate and boreal forests. Plant, Cell & Environment, 22(6), pp.715-740.

Malhi, Y., Wood, D., Baker, T.R., Wright, J., Phillips, O.L., Cochrane, T., Meir, P., Chave, J., Almeida, S., Arroyo, L. and Higuchi, N., 2006. The regional variation of aboveground live biomass in old-growth Amazonian forests. Global Change Biology, 12(7), pp.1107-1138.

Mascaro, J., Asner, G.P., Dent, D.H., DeWalt, S.J. and Denslow, J.S., 2012. Scale-dependence of aboveground carbon accumulation in secondary forests of Panama: a test of the intermediate peak hypothesis. Forest Ecology and Management, 276, pp.62-70.

McDade, L.A., Bawa, K.S., Hespenheide, H.A. and Hartshorn, G.S., 1994. La Selva, ecology and natural history of a Neotropical rain forest. University of Chicago Press, Chicago.

Myers, N., Mittermeier, R.A., Mittermeier, C.G., Da Fonseca, G.A. and Kent, J., 2000. Biodiversity hotspots for conservation priorities. *Nature*, *403*(6772), pp.853-858.

Morel, A.C., Saatchi, S.S., Malhi, Y., Berry, N.J., Banin, L., Burslem, D., Nilus, R. and Ong, R.C., 2011. Estimating aboveground biomass in forest and oil palm plantation in Sabah, Malaysian Borneo using ALOS PALSAR data. Forest Ecology and Management, 262(9), pp.1786-1798.

Myers, N., Mittermeier, R.A., Mittermeier, C.G., Da Fonseca, G.A. and Kent, J., 2000. Biodiversity hotspots for conservation priorities. Nature, 403(6772), pp.853-858.

Oberbauer, S.F. and Strain, B.R., 1984. Photosynthesis and successional status of Costa Rican rain forest trees. Photosynthesis Research, 5(3), pp.227-232.

O'Brien, S.T., Hubbell, S.P., Spiro, P., Condit, R. and Foster, R.B., 1995. Diameter, height, crown, and age relationship in eight neotropical tree species. Ecology, 76(6), pp.1926-1939.
Perry, D.A., 1994. Forest Ecosystems. John Hopkins University Press, Baltimore, MD, 649pp.

Perry, D.A., 1994. Forest Ecosystems. John Hopkins University Press, Baltimore, MD, 649 pp.

Popescu, S.C., 2007. Estimating biomass of individual pine trees using airborne lidar. Biomass and Bioenergy, 31(9), pp.646-655.

Potter, C., Klooster, S. and Genovese, V., 2009. Carbon emissions from deforestation in the Brazilian Amazon region predicted from satellite data and ecosystem modeling. Biogeosciences Discussions, 6(2).

Pretzsch, H., 2009. Forest dynamics, growth, and yield. In Forest Dynamics, Growth and Yield (pp. 1-39). Springer Berlin Heidelberg.
Richards, P. W. 1996. The Tropical Rain Forest. 2nd edition. Cambridge University Press: Cambridge.

Ryan, M.G., Hubbard, R.M., Clark, D.A. and Sanford, R.L., 1994. Woody-tissue respiration for Simarouba amara and Minquartia guianensis, two tropical wet forest trees with different growth habits. Oecologia, 100(3), pp.213-220.

Rödig, E., Cuntz, M., Rammig, A., Fischer, R., Taubert, F. and Huth, A., 2018. The importance of forest structure for carbon fluxes of the Amazon rainforest. Environmental Research Letters, 13(5), p.054013.

Saatchi, S.S., Houghton, R.A., Dos Santos Alvala, R.C., Soares, J.V. and Yu, Y., 2007. Distribution of aboveground live biomass in the Amazon basin. Global Change Biology, 13(4), pp.816-837.

Saatchi, S.S., Harris, N.L., Brown, S., Lefsky, M., Mitchard, E.T., Salas, W., Zutta, B.R., Buermann, W., Lewis, S.L., Hagen, S. and Petrova, S., 2011a. Benchmark map of forest carbon stocks in tropical regions across three continents. Proceedings of the national academy of sciences, 108(24), pp.9899-9904.

Saatchi, S., Marlier, M., Chazdon, R.L., Clark, D.B. and Russell, A.E., 2011b. Impact of spatial variability of tropical forest structure on radar estimation of aboveground biomass. Remote Sensing of Environment, 115(11), pp.2836-2849.

Shugart, H.H., 1984. A theory of forest dynamics. The ecological implications of forest succession models. Springer-Verlag.

Shugart, H.H., 1998. Terrestrial ecosystems in changing environments. Cambridge University Press.

Shugart, H.H. 2003. A Theory of Forest Dynamics: The Ecological Implications of Forest Succession Models. Blackburn Press. Caldwell, New Jersey. 278 pp.

Shugart, H.H., Asner, G.P., Fischer, R., Huth, A., Knapp, N., Le Toan, T. and Shuman, J.K., 2015. Computer and remote-sensing infrastructure to enhance large-scale testing of individual-based forest models. Frontiers in Ecology and the Environment, 13(9), pp.503-511.

Shugart, H.H., Wang, B., Fischer, R., Ma, J., Fang, J., Yan, X., Huth, A. and Armstrong, A.H., 2018. Gap models and their individual-based relatives in the assessment of the consequences of global change. Environmental Research Letters, 13(3), p.033001.

Tang, H., Dubayah, R., Swatantran, A., Hofton, M., Sheldon, S., Clark, D.B. and Blair, B., 2012. Retrieval of vertical LAI profiles over tropical rain forests using waveform lidar at La Selva, Costa Rica. Remote Sensing of Environment, 124, pp.242-250.

Weishampel, J.F., Ranson, K.J. and Harding, D.J., 1996. Remote sensing of forest canopies. Selbyana, pp.6-14.

Zheng, D., Rademacher, J., Chen, J., Crow, T., Bresee, M., Le Moine, J. and Ryu, S.R., 2004. Estimating aboveground biomass using Landsat 7 ETM+ data across a managed landscape in northern Wisconsin, USA. Remote sensing of environment, 93(3), pp.402-411.